

# Statistical Relationships between Solar, Interplanetary, and Geomagnetic Disturbances, 1976–2000: 2

Yu. I. Yermolaev and M. Yu. Yermolaev

Space Research Institute, Russian Academy of Sciences, ul. Profsoyuznaya 84/32, Moscow, 117997 Russia

Received December 5, 2002

**Abstract**—In this paper we continue the analysis of the influence of solar and interplanetary events on magnetospheric storms that was started in [1]. Two data sets are additionally analyzed in the present study: solar flares of importance M5 and greater in 1976–2000 and halo CMEs observed by the *SOHO* spacecraft during the period of 1996–2000. It is demonstrated that the statistical characteristics of the new set of flares and of that analyzed before in [1] differ little, while the geoeffectiveness of the halo CMEs turned out to be much less than that of the previously published CMEs.

## INTRODUCTION

In our previous paper [1] we analyzed the relation between geomagnetic storms and interplanetary and some solar events for the 25-year observation period from 1976 to 2000. We used the following data available via the Internet: the solar wind (SW) plasma parameters (velocity, temperature, and ion density) and three components of the interplanetary magnetic field (IMF) (<http://nssdc.gsfc.nasa.gov/>) to analyze interplanetary disturbances and the hourly  $D_{st}$  indices (<http://nssdc.gsfc.nasa.gov/> and <http://swdcdb.kugi.kyoto-u.ac.jp/dstdir/>) to analyze geomagnetic storms over the 1976–2000 period. Out of the solar data, we analyzed a list of the strong solar X-ray flares (of importance M0 and greater) that revealed themselves in the enhancements of solar cosmic rays (SCRs) near the Earth (<http://sec.noaa.gov/ftplib/indices/SPE.txt>) and also the published data on coronal mass ejections (CMEs) [2, 3]. Since disturbances are transported from the Sun to the Earth mainly by the solar wind, some geoeffective solar flares could be omitted in the analyzed list. In the present study, we consider other sets of solar data: those on solar flares and on coronal mass ejections. In the first case, we consider all flares of importance M5 and higher ([ftp://ftp.ngdc.noaa.gov/STP/SOLAR\\_DATA/SOLAR\\_FLARES/XRAY\\_FLARES](ftp://ftp.ngdc.noaa.gov/STP/SOLAR_DATA/SOLAR_FLARES/XRAY_FLARES)) and as many as 653 flares of this kind were selected. As to the data on the coronal mass ejections, systematic CME catalogs are available for the *SOHO* observatory data starting from 1996 ([http://cdaw.gsfc.nasa.gov/CME\\_list/](http://cdaw.gsfc.nasa.gov/CME_list/)), and, therefore, we have analyzed the 5-year (1996–2000) observations with LASCO and EIT instruments on *SOHO* spacecraft considering only so-called halo CMEs; that is, the CMEs that occupy the entire area around the Sun in images, thus indicating that the ejection moves towards an observer, to the Earth. There were 125 recorded events of this type.

The goal of the present paper is to analyze the new data sets in the same manner as was done in the previous paper and to compare the obtained statistical characteristics.

## RESULTS

The variations of annual means of the sunspot number, of the numbers of solar flares for both sets, and of the number of magnetic storms are shown in Fig. 1. The numbers of strong flares and strong storms reach their maximums in the years of maximal solar activity. It is noteworthy that curves 2, 3, and 4 have fairly similar

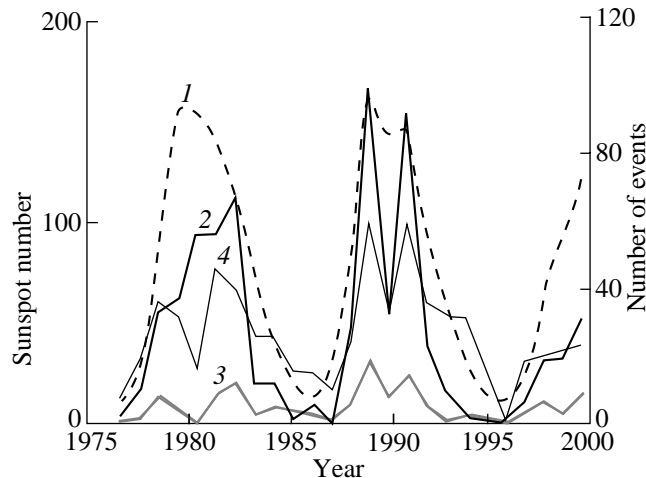


**Fig. 1.** Temporal variations of annual mean values of the sunspot number (curve 1, the scale on the left), the number of strong (importance M5 and higher) solar flares (curve 2, the scale on the right), the number of strong flares with SCR enhancements (with importance M0 and higher) (curve 3, the scale on the right), and the number of strong magnetic storms with the values of the  $D_{st}$  index in the minimum of less than  $-60$  nT (curve 4, the scale on the right).

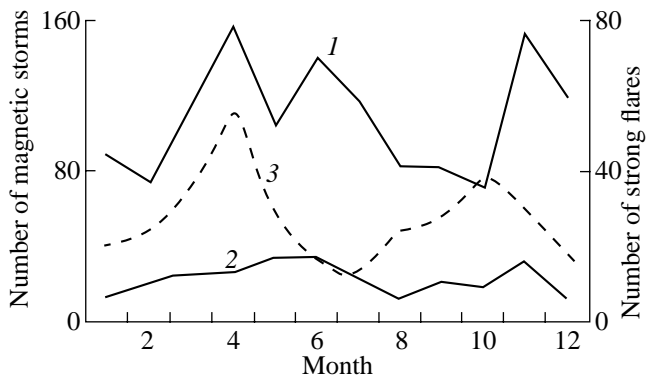


**Fig. 2.** Monthly distributions of the number of strong solar flares (curve 1) and flares with SCRs (curve 2) and of the number of strong magnetic storms (curve 3) as obtained by the method of epoch superposition for the period of 1976–2000.

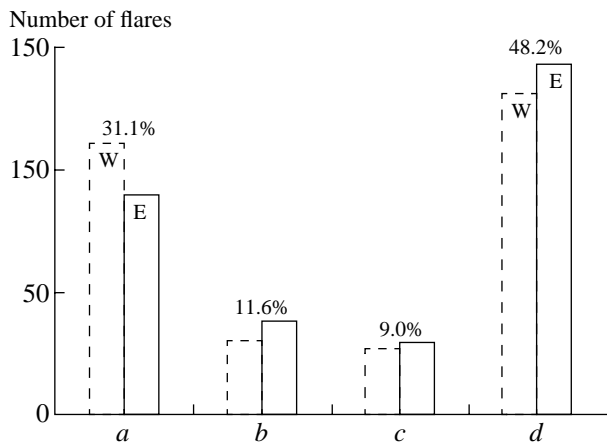


**Fig. 3.** The number of western and eastern strong solar flares (dashed and solid lines) that were (a) evidently, (b) probably, and (c) unlikely followed and (d) not followed by magnetic storms.

shapes (the correlation coefficients for the pairs of curves 2–4 and 3–4 are  $\sim 0.8$  and  $\sim 0.9$ , respectively) thus indicating that the variations of the flare and magnetic storm numbers can have one common cause. However, we show below that magnetic storms proved to be nearly unrelated to solar flares.

Monthly distributions of the number of solar flares for both sets and of the number of magnetic storms were obtained by the method of epoch superposition and are demonstrated in Fig. 2. Two maxima in the distribution of magnetic storms, in spring and in autumn, confirm the Russell–McPherron effect [4], which is associated with the annual evolution of the inclination of the Earth’s rotation axis with respect to the Sun–Earth line. The monthly distributions of flares are different both in the number of maxima (three for strong flares and two for flares with SCRs) and in their positions; and for both sets the positions of the maxima do

not coincide with those for the magnetic storms. Thus, the figure demonstrates that there is no correlation between flares and magnetic storms on a scale of about one month.

In our previous study [1] we associated the flares that manifested themselves in the SCR near the Earth with the storms by the following algorithm. If an SW disturbance (or a minimum in the  $D_{st}$  index, if the disturbance type could not be defined) was observed two–four days after a flare, this flare was considered as a potential candidate for the solar source of the storm; the flare was considered probable if it occurred within the extended time interval of 1.5–5 days (that is, within two subintervals, 1.5–2 and 4–5 days); it was assumed to have a low probability if it happened within a 1–6 day interval (1–1.5 and 5–6); and it was considered improbable if it did not fall within the last interval at all. It should be noted that the time of 2–4 days corresponds to the average velocity of propagation along the Sun–Earth path equal to 430–870 km/s, which is the usual SW velocity at the Earth’s orbit. A similar analysis was also performed for the full set of solar flares of importance M5 and higher. The results of this analysis are given in the form of bar charts in Fig. 3, where dashed and solid lines correspond to western and eastern flares, respectively, and the bar charts *a*, *b*, *c*, and *d* correspond to the evident sources of storms (31.1%, 25.4% for flares with SCR), to the probable (11.6% and 18.3%) and low-probability (9.0% and 19.0%) ones, and to the flares that did not result in a storm (48.2% and 37.3%), respectively. The differences between the two sets are small and are revealed in higher values in groups *a* and *d*, with lower values in groups *c* and *b* for the large set.

As can be seen from Fig. 4, the distributions of all types of flares, *a*, *b*, *c*, and *d*, over the solar disk are nearly the same and flares of all types are observed in wide ranges of solar latitudes and longitudes. For the two sets of flares in their entirety, the total number of the eastern flares proved to be somewhat greater than that of the western ones. However, after normalizing the number of both types of flares, the difference between the fractions of western and eastern flares in all bar charts practically disappears.

For the flares of the first three groups, we studied the dependence of the minimum of the  $D_{st}$  index during a storm on the flare importance (that is, on the flux of X-ray emission or energy) both for strong flares (upper panel) and for flares with SCRs (lower panel). Figure 5 demonstrates this dependence; circles, triangles, and diamonds correspond to evident, probable, and low-probability sources, and empty and solid symbols stand for western and eastern flares, respectively. No dependence of the storm strength on the flare energy is seen in the figure, neither for the two sets of flares in total nor for any selected flare subclass, though the X-ray flux for the flares given in the figure varies by two-and-a-half orders of magnitude. It is interesting that there is no one strong storm with a  $D_{st}$  index below  $-100$  nT asso-

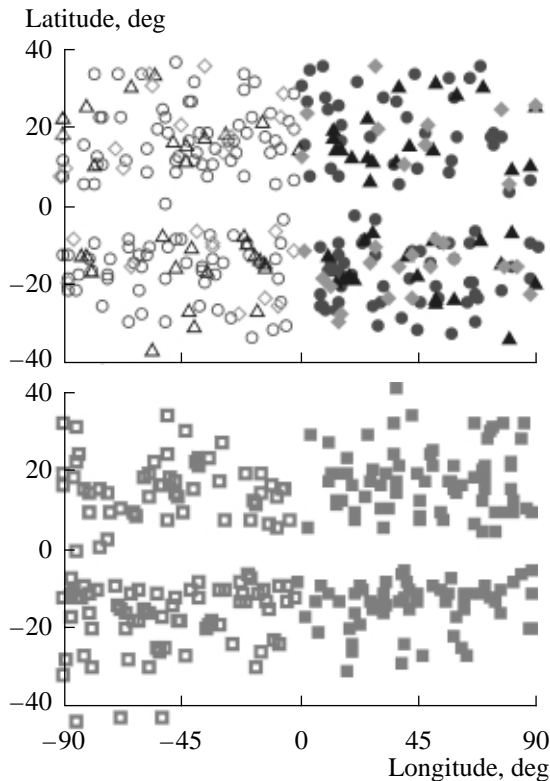


**Fig. 4.** Upper panel: the location of strong geoeffective flares on the solar disk; circles, triangles, and diamonds correspond to the *a*, *b*, and *c* type events. Lower panel: the location of nongeoeffective strong flares, the events of type *d* (see text).

ciated with the strongest flares in both panels, while for flares with a lower importance the storms are observed with a  $D_{st}$  index of  $\sim -300$  nT and lower. Among strong flares with SCRs, there are no possible candidates for the source of the storm of March 14, 1989, which was the strongest during the 25-year period analyzed. Meanwhile, as many as three candidates are found among the other flares with importance from X1 to X5. This means that, judging from the time lag, the three flares can be candidates for the source of this storm or that it was their total effect that resulted in the strongest storm.

We investigated the relationship between the  $D_{st}$  minimum during a storm and the time  $T$  of the disturbance propagation from the Sun to the Earth. This relationship is demonstrated in Fig. 6. No clear dependence of the storm strength on the transport velocity is observed: a very weak dependence  $D_{st}$  (nT) =  $0.15 \times T(\text{h}) - 117$  is obtained from a 224-point approximation.

If we perform similar (but inverted in time) data “interpolation” starting not from the moments of strong solar flares, but from the moments of strong magnetic storms with  $D_{st} < -100$  nT, we find that 15% of the strong flares are evident candidates for the storm source, 5% are probable sources, 5% are low-probability sources, and no strong flares can be associated with

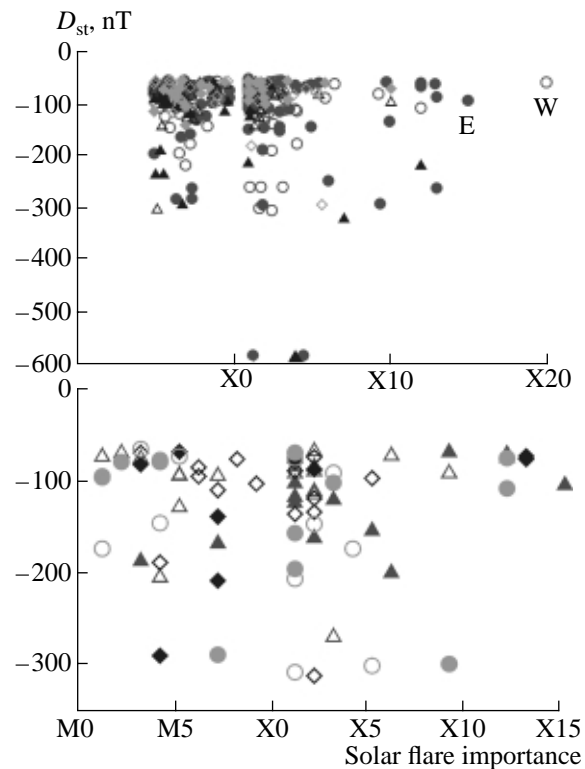


**Fig. 5.** The minimum of the  $D_{st}$  index during magnetic storms versus the X-ray importance (energy flux) of strong solar flares (upper panel) and of flares with SCRs (lower panel). Notation: empty and solid symbols correspond to western and eastern flares; circles, triangles, and diamonds mark the events of types *a*, *b*, and *c*.

75% of the strong storms (for the stronger storms with  $D_{st} < -200$  nT the corresponding values are 25%, 12%, 10%, and 53%; but for such storms the statistic is low, 32 storms).

Conflicting results follow from the analysis of the geoeffectiveness of another powerful solar disturbance, coronal mass ejections (CMEs), on the basis of the published data sets and the 1996–2000 set presented in the *SOHO* data base (see Introduction). On one hand, we have analyzed the list of CMEs [3] observed by the coronagraph on the *SOHO* space observatory and detected on the *WIND* spacecraft as MCs. The results of this analysis show that 16 (57%) of such CMEs (out of 28) resulted in moderate and strong magnetic storms; 10, in moderate storms with  $D_{st}$  from  $-60$  to  $-100$  nT; and 6, in strong storms with  $D_{st} < -100$  nT. On the basis of the 1975–1983 photometer data of the *HELIOS-1*, 2 spacecraft, 38 CMEs moving along the Sun–Earth line were detected in [4]. Using the estimates of the time of CME propagation from the Sun to the Earth and analyzing the level of magnetospheric disturbance by the  $K_p$  index, the author found that half of the CMEs (19) led to storms, 13 CMEs did not, and it was difficult to make any definite conclusion for 6 CMEs. It can be assumed that some of these six CMEs were, neverthe-

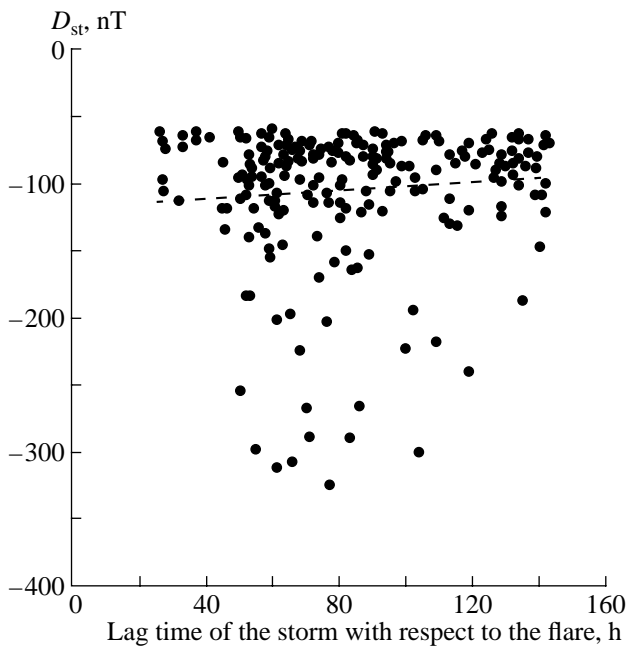


**Fig. 6.** The minimum of the  $D_{st}$  index during the storm versus the lag time of the storm with respect to the solar flare. The dashed line shows the approximation of the data presented.

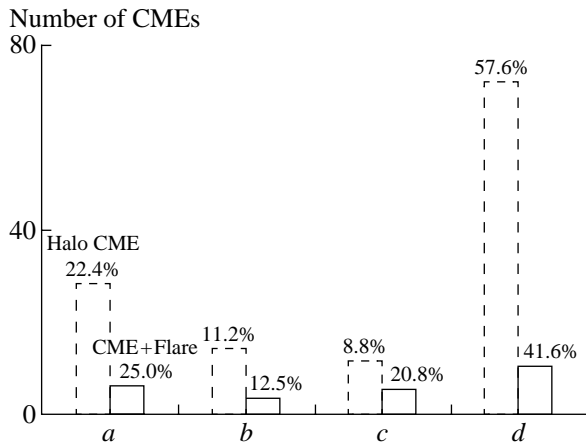


**Fig. 7.** The number of CMEs (dashed line) and the number of the flare-associated CMEs (solid line) that were (a) evidently, (b) probably, and (c) unlikely followed and (d) not followed by magnetic storms.

less, geoeffective. Therefore, the estimate of  $\sim 60\%$  for the fraction of geoeffective CMEs, which was obtained from two different samples for three various spacecraft, can be considered as well substantiated.

On the other hand, there are 125 so-called halo CMEs in the CME set detected at the *SOHO* observatory in 1996–2000. These are the CMEs that occupy the entire area around the Sun in the images and, as it is assumed, move towards an observer, to the Earth.

Twenty-four such CMEs were accompanied by strong flares from the described set of strong flares. Applying the above-described method for defining the possible geoeffectiveness from the CME-magnetic storm time lag, we found a low geoeffectiveness of the CMEs (see Fig. 7). It is 22.4% and 25.0% for type *a*, 11.2% and 12.5% for type *b*, 8.8% and 20.8% for type *c*, 57.6% and 41.6% for type *d* for all CMEs and for the flare-associated CMEs, respectively. The obtained CME geoeffectiveness turned out to be not only lower than that of the published CME sets, but even smaller than the geoeffectiveness of the solar flares. The differences between our estimates of the CME geoeffectiveness and the published data are, apparently, associated with the preliminary selection of the events before publications.

## DISCUSSION AND CONCLUSIONS

In our previous study [1], assuming that both solar events and storms occur in a random way, we estimated the probability of storm observation as the ratio of the length of the lag “window” between solar and terrestrial events of 3.5 days (from 1.5 to 5 days) to the average interval between the storms of 8–10 days. This estimate shows that, even for the random distribution of solar and terrestrial events, their “correlation” will be observed in 35–44% of cases. Thus, the geoeffectiveness of strong solar flares obtained for two flare sets (for all flares of importance M5 and higher and for all flares of importance M0 and higher accompanied by an increase in solar cosmic rays) can be partially or totally associated with random processes. This is also supported by the absence of a correlation of the importance of solar flares with the strength of magnetic storms (see Fig. 4), as well as with the propagation time (see Fig. 6).

The geoeffectiveness of the published CME data [2, 3] is higher; it exceeds the obtained threshold for random processes. However, our analysis of the halo CME data, recorded on the *SOHO* spacecraft in 1996–2000, demonstrates that the CMEs–magnetic storms correlation is low (about 35%) and can be of a random character.

## ACKNOWLEDGMENTS

The authors thank the international scientific centers SEC NOAA, NSSDC/GSFC NASA, and WDC-C2 for the information provided. They also thank L.M. Zelenyi, A.A. Petrukovich, and G.N. Zastenker for attention, help, and useful discussions on the subject matter of this paper. This study was supported in part by the Russian Foundation for Basic Research, project nos. 01-02-16182, 02-02-17160, 03-02-17474, 00-02-22001, and by APIC 0090 and INTAS 99-0078 grants.

## REFERENCES

1. Yermolaev, Yu.I. and Yermolaev, M.Yu., Statistical Relationships between Solar, Interplanetary, and Geomagnetic Disturbances, 1976–2000, *Kosm. Issled.*, 2002, vol. 40, no. 1, p. 3.
2. Gopalswamy, N., Lara, A., Lepping, R.P., *et al.*, Interplanetary Acceleration of Coronal Mass Ejections, *Geophys. Res. Lett.*, 2000, vol. 27, p. 145.
3. Webb, D.F., Jackson, B.V., and Hick, P., Geomagnetic Storms and Heliospheric CMEs as Viewed from HELIOS, in *Solar Drivers of Interplanetary and Terrestrial Disturbances*, *ASP Conference Series*, 1996, vol. 95, p. 167.
4. Russell, C.T. and McPherron, R.L., Semiannual Variation of Geomagnetic Activity, *J. Geophys. Res.*, 1973, vol. 78, p. 24.